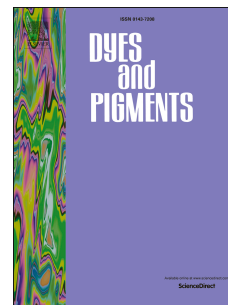


Accepted Manuscript

A simple water-soluble phenazine dye for colorimetric/ fluorogenic dual-mode detection and removal of Cu²⁺ in natural water and plant samples

Tai-Bao Wei, Bi-Rong Yong, Li-Rong Dang, You-Ming Zhang, Hong Yao, Qi Lin



PII: S0143-7208(19)30944-1

DOI: <https://doi.org/10.1016/j.dyepig.2019.107707>

Article Number: 107707

Reference: DYPI 107707

To appear in: *Dyes and Pigments*

Received Date: 26 April 2019

Revised Date: 9 July 2019

Accepted Date: 9 July 2019

Please cite this article as: Wei T-B, Yong B-R, Dang L-R, Zhang Y-M, Yao H, Lin Q, A simple water-soluble phenazine dye for colorimetric/ fluorogenic dual-mode detection and removal of Cu²⁺ in natural water and plant samples, *Dyes and Pigments* (2019), doi: <https://doi.org/10.1016/j.dyepig.2019.107707>.

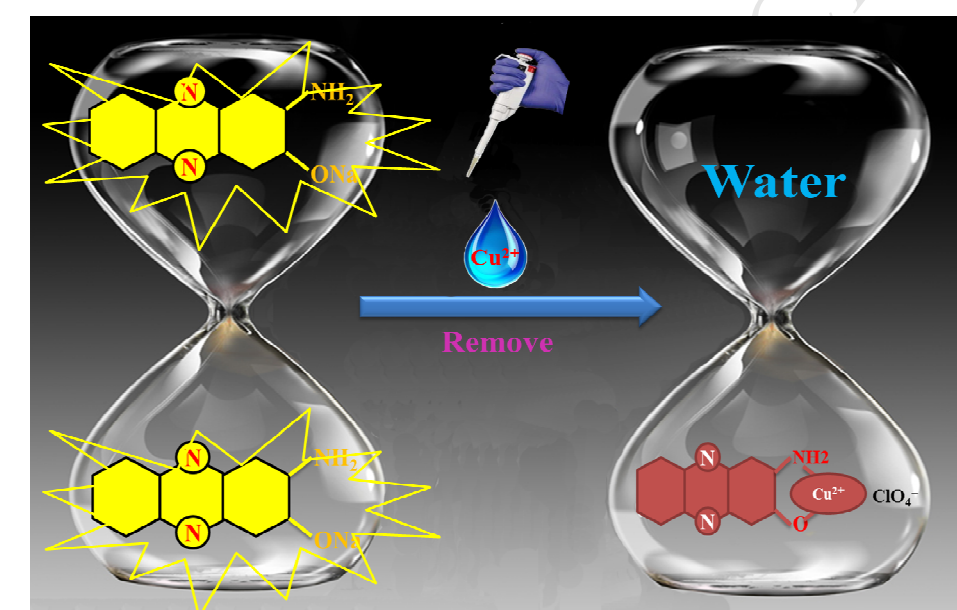
This is a PDF file of an unedited manuscript that has been accepted for publication. As a service to our customers we are providing this early version of the manuscript. The manuscript will undergo copyediting, typesetting, and review of the resulting proof before it is published in its final form. Please note that during the production process errors may be discovered which could affect the content, and all legal disclaimers that apply to the journal pertain.

Graphical Abstract

A simple water-soluble phenazine dye for colorimetric/ fluorogenic dual-mode detection and removal of Cu^{2+} in natural water and plant samples

Tai-Bao Wei ^{*a}, Bi-Rong Yong ^a, Li-Rong Dang ^a, You-Ming Zhang ^{a,b}, Hong Yao ^a and
Qi Lin ^{*a}

□



A rapid, low-cost, real-time and water-soluble phenazine dye (**AHPN**) was constructed for the colorimetric and fluorogenic detection of copper ions. At the same time, it shows excellent removal ability of copper ions in natural water samples.

* Corresponding authors. Tel.: +86-931-7973120; E-mail: weitaobao@126.com (T. - B. Wei); linqi2004@126.com (Q. Lin).

A simple water-soluble phenazine dye for colorimetric/ fluorogenic dual-mode detection and removal of Cu^{2+} in natural water and plant samples

Tai-Bao Wei ^{*a}, Bi-Rong Yong ^a, Li-Rong Dang ^a, You-Ming Zhang ^{a, b}, Hong Yao ^a and Qi Lin ^{*a}

^a Key Laboratory of Eco-Environment-Related Polymer Materials, Ministry of Education of China, Key Laboratory of Polymer Materials of Gansu Province,

College of Chemistry and Chemical Engineering, Northwest Normal University, Lanzhou, Gansu, 730070, P. R. China

^b College of Chemical and Chemical Engineering, Lanzhou City University, Lanzhou, Gansu, 730070, P. R. China.

Abstract

Detection and removal of heavy metal ions in a variety of complex water systems using dyes remains a challenge. Here we have developed a rapid, low-cost, on-site water-soluble dye for the colorimetric/fluorogenic detection and removal of copper ions in natural water and plant samples. By comparing with dye molecule AHP, this water-soluble phenazine dye (**AHPN**) has a high fluorescence quantum yield and excellent coordinated ability with copper ions. **AHPN** can effectively remove copper ions in various natural water samples due to its strong binding ability with Cu^{2+} . Moreover, the test strips also were fabricated and successfully used for real-time

* Corresponding authors. Tel.: +86-931-7973120; E-mail: weitaobao@126.com (T. - B. Wei); linqi2004@126.com (Q. Lin).

detection of Cu^{2+} in water with simple-to-use, low-cost, quick response and provide an obvious effect by naked-eye. All data in this experiment showed that this water-soluble phenazine dye **AHPN** has excellent effect on the detection and removal of Cu^{2+} .

Keywords: Water-soluble dye; Colorimetric/Fluorogenic; Detection; Removal; Cu^{2+} .

1. Introduction

Copper is the third most abundant transition metal in the human body [1]. It is also a micronutrient for all known life forms, and it has multiple functions ranging from bone formation and cellular respiration to connective tissue development [2-5]. Low level of Cu^{2+} in the cells will affect some enzymes activity, while Cu^{2+} existence in excess level will cause many diseases such as Wilson disease, Alzheimer disease, liver cirrhosis, prion-induced diseases and kidney failure [6-10]. High concentrations of Cu^{2+} can hamper the self-purification capability of the seas or rivers also can destroy the biological reprocessing systems in water; its toxicity can accumulate and non-biodegradable in the food chain, etc [11-16]. Cu^{2+} pollution has become more and more serious along with the development of industry. These problems are threatening the ecosystem and human health and have become a huge concern throughout the world [11].

Phenazine has a special status in the field of organic chemistry. Mid-19th century, Perkin tried to synthesize quinine but he got the mauveine (a mixture of substituted phenazine and other compounds) [17, 18]. This was the first time that humans had obtained a dyeable substance by chemical method, thus began a new era of artificial synthesis of dyes [19, 20]. There are also other applications those make phenazines attractive for modern chemistry [21], spanning from organic electronics to sensors and pharmaceutical purposes, as well as photoactive materials for dye sensitized solar cells and for photocatalysis [22-24].

Phenazine derivatives can be used as ion ligands and hydrogen bond receptors

due to their own structural characteristics (π system with electron deficiency, nitrogen atom with lone pair of electrons, and three condensed aromatic rings), and facilitate the cross-interaction of π - π electrons. Because of its large conjugate system, special optical properties, high fluorescence quantum yield, narrow emission band, large Stokes displacement and the maximum absorption and emission wavelength in the visible region [25-27]. Therefore, these compounds have great application prospects in the field of weak interaction in supramolecular chemistry, and they have been studied for many years as a molecular probe and molecular self-assembly device of signal response [28, 29]. In recent years, the application of phenazine derivatives are widely concerned in the field of molecular ion recognition and supramolecular self-assembly [30-32]. Therefore, it is of great significance to study the optical properties and sensing behavior of water-soluble phenazine dye.

Although there have been a lot of reports on the detection of copper ion [33-41] and application of dye [42-46], there are few reports on the detection and removal of copper ions in real water samples by phenazine dyes [47-48] (**Table S1**). In this work, we reported the water-soluble phenazine (**AHPN**) by colorimetric and fluorogenic detection and removal of Cu^{2+} . We treated it with NaOH to increase its solubility and optical properties [49]. At the same time, its application and difference with **AHP** optical response are also studied. This water-soluble phenazine dye has a higher fluorescence quantum yield (Φ up to 0.52) than **AHP** due to the intramolecular charge transfer from **AHP** to **AHPN**. It can also detect and remove Cu^{2+} in more complex natural water systems with low detection limit, quick response, and good

anti-interference ability. World Health Organization (WHO) and U. S. Environmental Protection Agency (EPA) had defined the concentration limits (2.0 mg/L and 1.3 mg/L) of copper in the drinking water [50]. In the three concentrations of solutions prepared by us, the worst adsorption concentration limits can reach 0.083 mg/L. Moreover, in order to make it more valuable, a colorimetric strip paper was fabricated. The fabricated test strip is simple-to-use, low-cost, instant and easily noticeable by naked-eye detection. This test strip also demonstrated excellent selectivity towards Cu^{2+} without interfering with any other ions. These data show that this water-soluble phenazine dye has a superior detection and high removal capacity for Cu^{2+} . Up to now, to the best of our knowledge, this is the first report on colorimetric and fluorescent chemosensor based on water-soluble phenazine dye for the detection and removal of Cu^{2+} in complex natural water systems.

2. Experimental section

2.1.1 Synthesis of dye molecule AHP

Diluted hydrochloric acid (6 mol/L) was added slowly to O-phenylenediamine (5.40 g, 50 mmol) in round-bottom flask (500 mL). The resulting solution was stirred at room temperature until the o-phenylenediamine completely dissolved. 53.0 g $\text{FeCl}_3 \cdot 6\text{H}_2\text{O}$ was dissolved in distilled water (75 mL) and trickled slowly into the round-bottom flask with a constant pressure funnel. With the addition of $\text{FeCl}_3 \cdot 6\text{H}_2\text{O}$, a red solid gradually formed. Produced mixture was stirred for 24 hours, then removed and filtered, the red solid was washed with 6mol/L diluted hydrochloric acid for 3 to 5 times. Put red solid in hot distilled water at 100°C and added 75 ml NaOH

(2 mol/L) into it, then a yellow solid is formed immediately. Continue to stir for 30 to 35 minutes and let it stand for 12hrs, after the suction filtration has tan solid was produced which was 2,3-diaminophenazine (Yield: 41.5%). An orange precipitate was formed gradually after the addition of hydrochloric acid to the filtrate drop by drop. Then, adjust the appropriate pH (pH=4~5) for precipitate and washed with distilled water. The obtained orange-red solid after drying was 2-amino-3-hydroxyphenazine (**AHP**). The reaction mechanism and synthesis route of **AHP** were showed in **Scheme S1**. Yield: 52.7%. m.p > 300°C; ¹H NMR (DMSO-*d*₆, 600 MHz) δ: 11.33 (s, 1H), 7.94 (dd, *J* = 17.8, 7.7 Hz, 2H), 7.60 (m, 2H), 7.15 (s, 1H), 6.92 (s, 1H), 6.25 (s, 2H) [51-52].

2.1.2 Synthesis of dye molecule **AHPN**

The 2-amino-3-hydroxyphenazine (**AHP**) (0.4221 g, 2 mmol) was added to 20 ml of EtOH and stirred for 10 minutes in a magnetic stirrer until completely dissolved. Then, NaOH (0.08 g, 2 mmol) was added and brown precipitate was formed immediately. Stirring was continued to complete the precipitation, and filtered off the precipitate. Washed the precipitate with ethanol for 3 times and then dried it in oven (60°C). **AHPN** is a brown solid, it has a good solubility in distilled water. Yield: 98%. m.p > 300°C; ¹H NMR (DMSO-*d*₆, 600 MHz) δ: 7.63 (d, *J* = 8.2 Hz, 2H), 7.57 (s, 1H), 7.28-7.24 (m, 2H), 7.17 (m, 1H), 6.51 (s, 1H), 6.07 (s, 1H); ¹³C NMR (DMSO-*d*₆, 150 MHz), δ/ppm: 166.44, 150.61, 146.03, 143.58, 140.45, 138.82, 127.55, 126.88, 125.11, 123.42, 100.96, 98.27; IR: (KBr, cm⁻¹) ν: 3445 (NH₂), 3049 (ArH), 1538 (C=C), 1447 (C=C), 1222 (C-O); ESI/MS: *m/z* calcd for C₁₂H₈N₃NaO (M⁺) 233.0565,

found 233.0585 (Fig. S1 to Fig. S5). The synthetic route and structures of AHP and dye molecular AHPN are showed in Scheme 1.

2.2 Characterizations

2.2.1 General procedure for UV-vis experiments

All the UV-vis experiments were carried out in fresh double distilled water on a Shimadzu UV-2550 spectrometer. Any changes in the UV-vis spectra of the synthesized compound were recorded on addition of perchlorate salts while keeping the ligand concentration constant (2.0×10^{-5} M) in all experiments. Perchlorate salt of cations (Fe^{3+} , Hg^{2+} , Ag^+ , Ca^{2+} , Cu^{2+} , Co^{2+} , Ni^{2+} , Cd^{2+} , Pb^{2+} , Zn^{2+} , Cr^{3+} , Mg^{2+} and Fe^{2+}) were prepared with 4.0×10^{-4} M throughout all UV-vis experiments.

2.2.2 General procedure for fluorescence spectra experiments

All the fluorescence spectroscopy was carried out in fresh double distilled water on a Shimadzu RF-5301 spectrometer. Any changes in the fluorescence spectra of the synthesized compound were recorded on addition of perchlorate salts while keeping the ligand concentration constant (2.0×10^{-5} M) in all experiments. Perchlorate salt of ions (Fe^{3+} , Hg^{2+} , Ag^+ , Ca^{2+} , Cu^{2+} , Co^{2+} , Ni^{2+} , Cd^{2+} , Pb^{2+} , Zn^{2+} , Cr^{3+} , Mg^{2+} and Fe^{2+}) were prepared with 4.0×10^{-4} M throughout all fluorescence experiments.

2.2.3 General procedure for ^1H -NMR experiments

For ^1H NMR titrations, two stock solutions were prepared in $\text{DMSO-}d_6$. Aliquots of the two solutions were mixed directly in NMR tubes. Cu^{2+} was prepared with 0.01 mol/L in ^1H NMR titrations experiments.

2.2.4 Adsorption experiment

The concentration of **AHPN** and Cu^{2+} with 1×10^{-4} M, 1×10^{-5} M and 1×10^{-6} M were prepared respectively. Added different concentrations of Cu^{2+} and let the solution stand still for 10 minutes. Then, separating the precipitate, the supernatant was assessed by inductively coupled plasma (ICP) analysis.

2.2.5 General procedure for test papers experiments

For Cu^{2+} test papers, the commercial source of paper was bought from the Hangzhou Xinhua Paper Industry Co., Ltd. Test strips were prepared by immersing filter papers into fresh double distilled water of **AHPN**. The test strips containing the chemosensor **AHPN** were utilized to detect Cu^{2+} .

3. Results and Discussion

3.1 Effect of pH

The pH was adjusted by adding HCl and NaOH dropwise to the **AHP**, and the fluorescence intensity of the solution at different pH values was measured (pH from 2 to 13). pH-Dependent fluorescence responses of **AHP** (2×10^{-5} M) in distilled water upon excitation at 450 nm was characterized in **Figure 2**. We can see it clearly, The pH is from 2 to 5, the fluorescence intensity showed a downward trend, the pH is from 6 to 13, and the fluorescence intensity is continuously increased.

Figure 1

In this context, we synthesized the sodium salts (**AHPN**) of **AHP**. The absorbance and fluorescence intensity of **AHP** and **AHPN** (2×10^{-5} M) in distilled water was characterized in **Fig. S6** and **Fig. S7**. We can clearly observe that the intensity of **AHPN** is the highest among them in both the emission spectrum and the

UV-vis absorption spectrum. The water-solubility of **AHP** and **AHPN** in water were calculated by the Lambert-Beer law. The **AHP** corresponding maximum concentration in ultraviolet titration experiment is 2×10^{-5} M, the **AHPN** corresponding maximum concentration in ultraviolet titration experiment is 2×10^{-4} M, so, **AHPN** has the best solubility in pure water (**Fig. S8** and **Fig. S9**). The emission quantum yield (Φ_1) of the **AHP** was calculated by 0.26 but **AHPN** can be up to 0.52 (Φ_2) (in Supporting Information). Therefore, it is more significant to study the recognition performance of **AHPN**. But in order to compare the difference in the recognition performance of metal ions between **AHP** and **AHPN**, the recognition performance of **AHP** with metal ions also be performed in supporting information (**Fig. S10** to **Fig. S16**).

3.1. UV-vis and fluorescence spectra study

Then, we carefully investigated the influence of metal ions on **AHPN** in distilled water. The addition and diffusion of water solutions of various metal ions, including Fe^{3+} , Hg^{2+} , Ag^+ , Ca^{2+} , Cu^{2+} , Co^{2+} , Ni^{2+} , Cd^{2+} , Pb^{2+} , Zn^{2+} , Cr^{3+} , Mg^{2+} and Fe^{2+} were prepared with 4.0×10^{-4} M in distilled water. As shown in inset of **Figure 2**, when adding 5 equiv. of Cu^{2+} and other metal ions into **AHPN**, the color of **AHPN** quickly changed from bright yellow to blood red under naked eye (within 3s). Before the addition of metal ions, **AHPN** solution in distilled water showed two bands at 258 and 440 nm in UV-vis spectroscopy, respectively. By the addition of 5.0 equiv. of metal ions to a solution of **AHPN**, only Cu^{2+} induced the formation of new obvious absorption bands at 260 and 443 nm. Meanwhile, a dramatically decrease of the

absorbance from 0.64 (a.u.) to 0.36 (a.u.) of **AHPN** in UV-vis spectroscopy, while other metal ions produced slight spectral responses.

Figure 2

In order to validate the selectivity of sensor **AHPN**, the UV-vis absorption spectra competitive complexation of **AHPN** was studied in **Fig. S17**. The results show that **AHPN** has strong anti-interference ability to detect Cu^{2+} , and other cations have no or weak influence in UV-vis absorption spectrum response.

In order to further explore fluorogenic sensing abilities of **AHPN** in distilled water, a series of fluorescence spectral was examined. In **Figure 3**, the free sensor **AHPN** showed a dramatically fluorescence at 555 nm. When various metal ions were added, only the addition of Cu^{2+} could significantly reduce the fluorescence intensity (from 133 a.u. to 51 a.u.). Moreover, only the addition of Cu^{2+} can quench the fluorescence of **AHPN** under irradiation with a UV lamp at 365 nm. We know that from competitive experiments, other metal ions have no or negligible effect on emissions of **AHPN**, but due to Fe^{3+} and Cu^{2+} are paramagnetic ions, there is some interference with each other. This idea was also proved by adding Fe^{2+} . As can be seen in **Fig. S18**, the addition of Fe^{2+} also has certain interference with Cu^{2+} , so this is confirmed.

Figure 3

To further examine the recognition behavior of the **AHPN** with Cu^{2+} , UV-vis spectrum and fluorescence titration experiment of **AHPN** also were studied in distilled water (**Fig. S19 to Fig. S22**). The detection limit of the UV-vis spectral and

fluorescence change is calculated on the basis of $3\delta/S$ method is 7.6×10^{-6} M and 2.2×10^{-7} M, respectively. The pH-dependent ultraviolet-visible and fluorescence spectrum experiments of **AHPN** and **AHPN**+ Cu^{2+} using the buffer solution were tested in **Fig. S23** and **Fig. S24**. Through experiments, we found that pH has no or only slight effect on **AHPN** for detection of Cu^{2+} in ultraviolet and fluorescence spectrum.

3.4. The naked-eye detection limit of **AHPN**

In addition, in order to investigate the naked-eye detection ability of **AHPN** in distilled water, we also tasted the naked-eye detection limit of **AHPN**. As shown in **Fig. S25**, the naked eye detection concentration of **AHPN** in visible light is 1×10^{-6} M. The naked-eye detection limit of **AHPN** under irradiation with the UV lamp also been tasted in **Fig. S26**. As can be seen from the figure, the detection concentration is also 1×10^{-6} M.

3.3. The binding mechanisms of **AHPN**

To further understand the nature of the stimuli-response mechanism between **AHPN** with Cu^{2+} , The ^1H NMR titration, IR, XRD, Mass spectra, Job's plot and SEM was carefully investigated [53-59]. The ^1H NMR titration experiments were performed in $\text{DMSO-}d_6$ with **AHPN** (0.05mol/L) in the existence of Cu^{2+} (0.01 mol/L), and the spectral details are shown in **Figure 4**. The addition of Cu^{2+} to **AHPN** in $\text{DMSO-}d_6$ solution directed a downfield shift of the signal of the hydrogen atoms in the phenazine rings (Ha, Hb, Hc, Hd) and amino proton $-\text{NH}_2$ (H_1 and H_2). Upon addition of Cu^{2+} to **AHPN**, the Ha protons were shifted from 7.62 to 7.71 ppm, Hb

protons were shifted from 7.57 to 7.65 ppm, Hc protons were shifted from 7.26 to 7.33 ppm, Hd protons were shifted from 7.17 to 7.26 ppm, H₁ protons were shifted from 6.50 to 6.62 ppm and H₂ protons were shifted from 6.07 to 6.27 ppm, respectively. The above results indicate that the **AHPN** coordinates with Cu²⁺. The Job's plot and mass spectral data revealed that the complex was formed between **AHPN** and Cu²⁺ in 1:1 stoichiometry (**Fig. S27**), the mass spectral also confirmed the formation of **AHPN** and Cu in **Fig. S5**.

Figure 4

The IR spectrum of **AHPN** and **AHPN-Cu** can elucidate the binding mode in **Fig. S28**. The IR spectra of **AHPN**, the stretching vibration absorption peaks of -NH₂ appeared at 3345 and 3480 cm⁻¹, -C-O appeared at 1088 cm⁻¹, respectively. However, when **AHPN** coordinated with Cu²⁺, the stretching vibration absorption peaks of imidazole -NH₂ intensity decreases, whereas the stretching vibration absorption peaks of -C-O intensity increased, which indicated that **AHPN** complex with Cu²⁺ via N-Cu-O coordination bond.

Based on the above results, we propose that the reaction mechanism and binding model of dye molecule **AHPN** with Cu²⁺ in **Figure 5**. To get further insight into the morphological features of the **AHPN** and **AHPN-Cu**, the XRD and SEM studies were carried out. In **Fig. S29**, there have two X-ray diffraction peaks at 7.3° and 12.1° in **AHPN**, which shows a distinct monomer. But this obvious diffraction peak disappeared is due to the formation of mixed ligand complexes with Cu²⁺. A peak at 17.5°, it showed the typical NH- π distance is 2.56Å, in curve of **AHPN-Cu**, this peak

gets weaker. It indicates that NH- π in **AHPN** gets weaker after combination with Cu^{2+} . A peak at 22.2° , the distance is 2.04 \AA , that the Cu-O bond's distance. At 24.7° , $d=1.80 \text{ \AA}$, it's the Cu-N distances in the **AHPN-Cu** complex. Two sharp diffraction peaks at 26.9° and 28° observed of **AHPN**, in the powder the XRD of **AHPN-Cu**, these peaks did not disappear but moved to 25.0° and 25.5° . This phenomenon shows that the **AHPN** coordinated with Cu^{2+} did not destroyed the π - π stacking between molecular of **AHPN**. In addition, the morphological features of **AHPN** and **AHPN-Cu** were studied using SEM, which showed an irregular rod-like structure before cooperating with Cu^{2+} . After the addition of Cu^{2+} , **AHPN** and Cu^{2+} coordinate with metal-coordination, leading to the destruction of hydrogen bonds in **AHPN** molecules, and weaken NH- π and π - π stacking interactions, so the original structure collapses into a laminar structure (**Fig. S30**).

Figure 5

3.7. Computational study

The optimized structure of **AHPN-Cu** and the HOMO-LUMO energy gaps for **AHPN** and **AHPN-Cu** were performed by DFT calculations. The proposed binding mechanism is verified by calculating the optimized structure of **AHPN** and **AHPN-Cu** (**Fig. S31**). The Frontline orbital energy map of **AHPN** and **AHPN-Cu** was showed in **Figure 6**. The HOMO-LUMO energy differences (ED) for **AHPN** and **AHPN-Cu** were found to be 0.04568 eV and 0.04365 eV respectively (The DFT calculations data of **AHPN** and **AHPN-Cu** were showed in **Table S2** and **Table S3**). This indicates that the energy of **AHP** is transferred after the addition of Cu^{2+} , and the

energy of **AHPN-Cu** is lower, and the fluorescence quenching occurs after the addition of Cu^{2+} . We speculate that it may be due to the presence of PET process.

Figure 6

3.6. Adsorption capacity of the AHPN

Adsorption capacity of the **AHPN** for Cu^{2+} in pure water was assessed inductively coupled plasma (ICP) analysis.

To test the suitability in practical applications, we also evaluated the performance of **AHPN** in the applicable removal of Cu^{2+} (**Figure 7**). The dye **AHPN** exhibited excellent solubility in pure water. When the concentration of the **AHPN** and Cu^{2+} were both 1×10^{-4} M, 1×10^{-5} M and 1×10^{-6} M respectively, Cu^{2+} were added to the host solution, the solution first changed from bright yellow to blood red. After 10 minutes, the red solution gradually became colorless with the formation of reddish-brown precipitation. The supernatant was tested by ICP, and it was found that Cu^{2+} was not detected in the supernatant at the concentrations of 1×10^{-4} M and 1×10^{-5} M. When the concentration is 1×10^{-6} M, Cu^{2+} is 0.083 mg/L in supernatant. The Cu^{2+} removal efficiency was displayed up to 76% (**Table S4**).

Figure 7

3.6. Application in real samples and plant samples

Meanwhile, the **AHPN** also was further subjected to natural water examples and paper strip test. Generally, the application of dye molecular detect and remove Cu^{2+} in natural water samples presents a unique set of challenges, which requires detailed studies of dye molecular performance in the environmental milieu. Next, we tested the

responding ability of **AHPN** to Cu^{2+} in several natural water samples (River water, lake water and snow water). As shown in **Fig. S32**, the fluorescence quenching of **AHPN** also produced the red-brown precipitate in each samples. These results clearly show that **AHPN** can detect Cu^{2+} in the solutions with a much more complicated composition. At the same time, as an application in plant samples, we took fresh aloe vera, peeled off a layer of skin, soaked it in **AHPN** solution, and then took it out and added Cu^{2+} (4×10^{-3} mol/L) onto the surface. We found that **AHPN** can completely enter the pulp of aloe vera before the addition of Cu^{2+} . After the addition of Cu^{2+} , the pulp's surface of aloe vera changed to blood red immediately. However, this blood red does not penetrate into the pulp inside, and will form a flocculation on the surface (**Fig. S33**). This phenomenon indicates that **AHPN** can be used to detect Cu^{2+} in plants.

To further realize the practical application, the **AHPN** was prepared as a test paper to evaluate its capability of detecting Cu^{2+} in water. In the experiment, the test papers were initially immersed in 2×10^{-4} M concentration of **AHPN** solution. After that, the test papers were added with Cu^{2+} . The color of the **AHPN**-based test papers rapidly changes from yellow to blood red in visible light. The fluorescence was quenched rapidly under irradiation with the UV lamp at 365 nm. And the minimum concentration of Cu^{2+} detected by this test strip in the naked eye was 1×10^{-6} M (**Fig. S34**). The solubility of **AHPN** coated on the surface of the test paper was also tested. We coated the **AHPN** on the strips and drip distilled water onto the surface of the test paper strips, it can see that the **AHPN** dissolved on the surface of the test paper strips

as it dripped distilled water. What's more, when the solid of **AHPN** was completely dissolved on the test paper, washing the test paper strip with distilled water repeatedly found that the dye had completely colored the test paper strip and did not fade (**Fig. S35**).

4. Conclusion

In summary, we reported a water-soluble dye based on phenazine for high-performance, dual-mode detection and removal of Cu^{2+} in water. This phenazine dye is simple and low-cost to synthesize. Moreover, as an application material, it not only can detect Cu^{2+} with quick response and high selectivity, but also can remove Cu^{2+} with rapid and high adsorption capacity in natural water samples. The test strips based on the **AHPN** also were fabricated and used to convenient detection of Cu^{2+} in water. Based on all the above studies we suggest that the water-soluble dye **AHPN** has great potential in the treatment of Cu^{2+} pollution in toxicology or environmental sciences.

Conflicts of interest

The authors declare no competing financial interests

Funding

This work was supported by the National Natural Science Foundation of China (Nos. 21662031; 21661028; 21574104), the Program for Changjiang Scholars and Innovative Research Team in University of Ministry of Education of China (IRT

15R56).

References

- [1] Xu YF, Hou YH, Wang YT, YF Wang, Li T, Song C, Wei NN, QF Wang. Sensitive and selective detection of Cu^{2+} ions based on fluorescent Ag nanoparticles synthesized by R-phycoerythrin from marine algae *Porphyra yezoensis*. *Ecotoxicol Environ Saf* 2019;168: 356-62.
- [2] Chen YC, Zhu CC, Cen JJ, Li J, He WJ, Jiao Y, ZJ Guo. A reversible ratiometric sensor for intracellular Cu^{2+} imaging: metal coordination-altered FRET in a dual fluorophore hybrid. *Chem Commun* 2013; 49: 7632-4.
- [3] Yin K, Li BW, Wang XC, Zhang WW, Chen LX. Ultrasensitive colorimetric detection of Cu^{2+} ion based on catalytic oxidation of l-cysteine. *Biosens Bioelectron* 2015; 15: 81-7.
- [4] Yin J, Bing QJ, Wang L, Wang G. Ultrasensitive and highly selective detection of Cu^{2+} ions based on a new carbazole-Schiff. *Spectrochim Acta Part A* 2018; 189: 495-501.
- [5] Zhang BB, Liu HY, Wu FX, Hao GF, Chen YZ, Tan CY, Tan Y, Jiang YY. A dual-response quinoline-based fluorescent sensor for the detection of Copper (II) and Iron(III) ions in aqueous medium. *Sens Actuators B* 2017; 243: 765-74.
- [6] Yang MD, Zhang Y, Zhu WJ, Wang HZ, Huang J, Cheng LH, Zhou HQ, Wu JY, Tian YP. Difunctional chemosensor for Cu(II) and Zn(II) based on Schiff base modified anthryl derivative with aggregation-induced emission enhancement and

- piezochromic characteristics. *J Mater Chem C* 2015; 3: 1994-2002.
- [7] Li W, Zhang Y, Gan XQ, Yang MD, Mie B, Fang M, Zhang QY, Yu JH, Wu JY, Tian YQ, Zhou HQ. A triphenylamine-isophorone-based “off-on” fluorescent and colorimetric probe for Cu^{2+} , *Sens Actuators B* 2015; 206: 640-646.
- [8] Sakunkaewkasem S, Petdum A, Panchan W, Sirirak J, Charoenpanich A, Sooksimuang T, Wanichacheva N. Dual-Analyte Fluorescent sensor based on [5] Helicene derivative with super large Stokes shift for the selective determinations of Cu^{2+} or Zn^{2+} in buffer solutions and its application in a living cell. *ACS Sens* 2018; 3: 1016-23.
- [9] Fan JL, Zhan P, Hu MM, Sun W, Tang JZ, Wang JY, Sun SG, Song FL, Peng XJ. A fluorescent ratiometric chemodosimeter for Cu^{2+} based on TBET and its application in living cells. *Org Lett* 2013; 15: 492-5.
- [10] Xu J, Wang ZK, Liu CY, Xu ZH, Zhu BC, Wang N, Wang K, Wang JT. A colorimetric and fluorescent probe for the detection of Cu^{2+} in a complete aqueous solution. *Anal Sci* 2018; 34: 453-7.
- [11] Xia Y, Zhang HH, Zhu XJ, Zhang GJ, Yang XY, Li F, Zhang XJ, Fang M, Yu JH, Zhou HP. A highly selective two-photon fluorescent chemosensor for tracking homocysteine via situ reaction, *Dyes Pigm* 2018; 155: 159-163.
- [12] Khatua S, Choi SH, Lee J, Huh JO, Do Y, Churchill DG. Highly selective fluorescence detection of Cu^{2+} in water by chiral dimeric Zn^{2+} complexes through direct displacement. *Inorg Chem* 2009; 48: 1799-801.
- [13] Xue XL, Fang HB, Chen HC, Zhang CL, Zhu CC, Bai Y, He WJ, Guo ZJ. In

vivo fluorescence imaging for Cu^{2+} in live mice by a new NIR fluorescent sensor.

Dyes Pigm 2016; 130: 116-21.

[14] Patil A, Salunke-Gawali S. Overview of the chemosensor ligands used for selective detection of anions and metal ions (Zn^{2+} , Cu^{2+} , Ni^{2+} , Co^{2+} , Fe^{2+} , Hg^{2+}).

Inorganica Chimica Acta 2018; 482: 99-112.

[15] Xia Y, Yu TT, Li F, Zhu WJ, Ji YG, Kong S, Li CX, Huang B, Zhang XJ, Tian YP, Zhou HP. A lipid droplet-targeted fluorescence probe for visualizing exogenous copper (II) based on LLCT and LMCT, Talanta 2018; 188: 178-182.

[16] Zhang X, Sun P, Li F, Li H, Zhou HP, Wang H, Zhang BW, Pan ZW, Tian YP, Zhang XJ. A tissue-permeable fluorescent probe for Al (III), Cu (II) imaging in vivo, Sens Actuators B 2018; 255: 366-373.

[17] Toshihiko T, Yutaka N, Haruo S, Kazuo Shin-ya. Phenazine derivatives. WO. 98247731 [P]. 1998-06-11.

[18] Miuer AG, Balchunis RJ. Phenazine dyes. US, 5428161 [P]. 1995-06-27.

[19] Bindewald E, Lorenz R, Hübner O, Brox D, Hertel DP, Kaifer E, Himmel HJ. Tetraguanidino-functionalized phenazine and fluorene dyes: synthesis, optical properties and metal coordination. Dalton Trans 2015; 44: 467.

[20] Koepf M, Lee SH, Brennan BJ, Méndez-Hernández DD, Batista VS, Brudvig GW, Crabtree RH. Preparation of halogenated fluorescent diaminophenazine building blocks. J Org Chem 2015; 80: 9881-8.

[21] Ou JG, Lu YH. Synthesis of α -phenazine carboxylic acid—a liquid light filter agent. Chem Reag 1982; 4: 41-3.

- [22] Cimmino A, Evidente A, Mathieu V, Andolfi A, Lefranc F, Kornienkod A, Kiss R. Phenazines and cancer. *Nat Prod Rep* 2012; 29: 487.
- [23] Krishnaiah M, Almeida NR, Udumula V, Song Z, Chhonker YS, Abdelmoaty MM, Nascimento VA, Murry DJ, Conda-Sheridan M. Synthesis, biological evaluation, and metabolic stability of phenazine derivatives as antibacterial agents. *Eur J Med Chem* 2018; 143: 936-47.
- [24] Gu PY, Wang ZL, Zhang QC. Azaacenes as active elements for sensing and bio application. *J Mater Chem B* 2016; 4: 7060-74.
- [25] Brombosz SM, Zuccherro AJ, Phillips RL, Vazquez D, Wilson A, Bunz UHF. Terpyridine-Based Cruciform-Zn²⁺ Complexes as Anion-Responsive Fluorophores. *Org Lett* 2007; 9: 4519-22.
- [26] Gill MR, Cecchin D, Walker MG, Mulla RS, Battaglia G, Smythe C, Thomas JA. Targeting the endoplasmic reticulum with a membrane-interactive luminescent ruthenium(II) polypyridyl complex. *Chem Sci* 2013; 4: 4512-9.
- [27] Yang L, Li X, Yang JB, Qu Y, Hua JL. Colorimetric and Ratiometric Near-Infrared Fluorescent Cyanide Chemodosimeter Based on Phenazine Derivatives. *ACS Appl Mater Interfaces* 2013; 5: 1317-26.
- [28] Ryazanova OA, Voloshin IM, Makitruk VL, Zozulya VN, Karachevtsev VA. pH-Induced changes in electronic absorption and fluorescence spectra of phenazine derivatives. *Spectrochim Acta Part A* 2007; 66: 849-859.
- [29] Pauliukaite R, Ghica ME, Barsan MM, Brett CMA. Phenazines and Polyphenazines in Electrochemical Sensors and Biosensors. *Anal Lett* 2010; 43: 1588-1608.

- [30] Abdelfattah MS, Kazufumi T, Ishibashi M. Izumiphenazines A-C: isolation and structure elucidation of phenazine derivatives from *Streptomyces* sp. IFM 11204. *Nat Prod* 2010; 73: 1999-2002.
- [31] Jana AK. Solar cells based on dyes. *J Photochem Photobiol A* 2000; 132:1-17.
- [32] Pauliukaite R, Ghica ME, Barsan MM, Brett CMA. Phenazines and polyphenazines in electrochemical sensors and biosensors. *Anal Lett* 2010; 43: 1588-1608.
- [33] Zhao Q, Yuan H, Xu XM, Hu L, Gong PW, Yan ZQ. A D- π -A- π -D organic conjugated molecule with multiple chelating points: Spectral property and its reversible visual sensing Cu²⁺. *Dyes Pigm* 2019; 165: 217-22.
- [34] Tian M, He H, Wang BB, Wang X, Liu Y, Jiang FL. A reaction-based turn-on fluorescent sensor for the detection of Cu (II) with excellent sensitivity and selectivity: Synthesis, DFT calculations, kinetics and application in real water samples. *Dyes Pigm* 2019; 165: 383-90.
- [35] Li DX, Sun X, Huang JM, Wang Q, Feng Y, Chen M, Meng XM, Zhu MZ, Wang X. A carbazole-based "turn-on" two-photon fluorescent probe for biological Cu²⁺ detection vis Cu²⁺-promoted hydrolysis. *Dyes Pigm* 2016; 125: 185-91.
- [36] Udhayakumari D, Velmathi S, Sung YM, Wu SP. Highly fluorescent probe for copper (II) ion based on commercially available compounds and live cell imaging. *Sens Actuators B* 2014; 198: 285-93.
- [37] Chang YX, Fu JX, Yao K, Li B, Xu KX, Pang XB. Novel fluorescent probes for sequential detection of Cu²⁺ and citrate anion and application in living cell imaging.

Dyes Pigm 2019; 161: 331-40.

[38] Yin Jun, Bing QJ, Wang L, Wang G. Ultrasensitive and highly selective detection of Cu^{2+} ions based on a new carbazole-Schiff. Spectrochim Acta Part A 2018; 189: 495-501.

[39] Li H, Zhang RL, Li CX, Huang B, Yu TT, Huang XD, Zhang XJ, Li F, Zhou HP, Tian YP. Real-time detection and imaging of copper (II) in cellular mitochondria. Org Biomol Chem 2017; 15: 598-604.

[40] Hwang SM, Kim C. Fluorescent detection of Zn^{2+} and Cu^{2+} by a phenanthrene-based multifunctional chemosensor that acts as a basic pH indicator. Inorg Chim Acta 2018; 482: 375-83.

[41] Kim MS, Jo TG, Yang M, Han J, Lim MH, Kim C. A fluorescent and colorimetric Schiff base chemosensor for the detection of Zn^{2+} and Cu^{2+} : Application in live cell imaging and colorimetric test kit. Spectrochim Acta Part A 2019; 211: 34-43.

[42] Park JS, Jeong S, Lee SDM, Song C. Colorimetric sensing of Cu^{2+} using a cyclodextrine-dye rotaxane. Dyes Pigm 2010; 87: 49-54.

[43] Chen YF, Tang TX, Chen YH, Xu DM. Novel 1,8-naphthalimide dye for multichannel sensing of H^+ and Cu^{2+} . Res Chem Intermed 2018; 44: 2379-293.

[44] Zhang Y, Wang YT, Kang XX, Ge M, Feng HY, Han J, Wang DH, Zhao DZ. Azobenzene disperse dye-based colorimetric probe for naked eye detection of Cu^{2+} in aqueous media: Spectral properties, theoretical insights, and applications. J Photochem Photobiol A 2018; 356: 652-60.

- [45] Sonawane M, Sahoo SK, Singh J, Singh N, Sawant CP, Kuwar A. A lawsone azo dye-based fluorescent chemosensor for Cu^{2+} and its application in drug analysis. *Inorg Chim Acta* 2015; 438: 37-41.
- [46] Dey N, Kulhanek J, Bureš F, Bhattacharya S. Simultaneous detection of Cu^{2+} and Hg^{2+} via two mutually independent sensing pathways of biimidazole push-pull dye. *J Org Chem* 2019; 84: 1787-96.
- [47] Aggarwal K, Khurana JM. Phenazine containing indeno-furan based colorimetric and “on–off” fluorescent sensor for the detection of Cu^{2+} and Pb^{2+} . *J Lumin* 2015; 167: 146-55.
- [48] Thangadurai TD, Nithya I, Rakkiyanasamy A. Development of three ways molecular logic gate based on water soluble phenazine fluorescent ‘selective ion’ sensor. *Spectrochim Acta Part A* 2019; 211: 132-40.
- [49] Jiang K, Ma S, Bi H, Chen D, Han X. Morphology controllable fabrication of poly-*o*-phenylenediamine microstructures tuned by the ionic strength and their applications in pH sensors. *J Mater Chem A* 2014; 2: 19208-13.
- [50] Zong CH, Ai KL, Zhang G, Li HW, Lu LH. Dual-emission fluorescent silica nanoparticle-based probe for ultrasensitive detection of Cu^{2+} . *Anal Chem* 2011; 83: 3126-32.
- [51] Amer AM, El-Bahnasawi AA, Mahran MRH. On the synthesis of pyrazino[2,3-*b*]phenazine and 1H-imidazo[4,5-*b*]phenazine derivatives, *Monatshefte Für Chemie* 2000; 31: 1217-25.
- [52] Korzhenevskii AB, Markova L, Efimova SV, Koifman OI, Krylova EV. Metal

complexes of a hexameric network tetrapyrazinoporpyrazine: i. synthesis and identification. *Russ J Gen Chem* 2005; 75: 980-4.

[53] Li ZY, Su HK, Zhou K, Yang BZ, Xiao TX, Sun XQ, Jiang JL, Wang LY. Oxo-spirocyclic structure bridged ditopic Schiff base: A turn-on fluorescent probe for selective recognition of Zn(II) and its application in biosensing. *Dyes Pigm* 2018; 149: 921-6.

[54] Tao JY, Sun D, Sun L, Li ZZ, Fu B, Liu J, Zhang L, Wang SF, Fang YY, Xu HJ. Tuning the photo-physical properties of BODIPY dyes: Effects of 1, 3, 5, 7-substitution on their optical and electrochemical behaviours. *Dyes Pigm* 2019; 167: 164-73.

[55] Zhu DJ, Ren AS, He XC, Luo YH, Duan ZH, Yan XW, Xiong YH, Zhong X. A novel ratiometric fluorescent probe for selective and sensitive detection of Cu²⁺ in complete aqueous solution. *Sens Actuators B* 2017; 252: 134-41.

[56] Ding ZY, Ma Y, Shang HX, Zhang HY, Jiang SM. Fluorescence Regulation and Photoresponsivity in AIEE Supramolecular Gels Based on a Cyanostilbene Modified Benzene-1,3,5-Tricarboxamide Derivative. *Chem Eur J* 2018; 24: 1- 9.

[57] Hatai J, Rahaman SA, Dasgupta D, Bandyopadhyay S. Instant detection of cyanide in seafood with a tryptophan based fluorescence probe. *Anal. Methods* 2019; <https://doi.org/10.1039/C9AY00936A>.

[58] Suo FT, Chen XW, Fang HX, Gong QY, Yu CM, Yang ND, Li S, Wu Q, Li L, Huang W. Hybrid fluorophores-based fluorogenic paper device for visually high-throughput detection of Cu²⁺ in real samples. *Dyes Pigm* 2019;

<https://doi.org/10.1016/j.dyepig.2019.107639>.

[59]Wang LY, Wu SM, Tang H, Meier H, Cao DR. An efficient probe for sensing different concentration ranges of glutathione based on AIE-active Schiff base nanoaggregates with distinct reaction mechanism. *Sens Actuators B* 2018; 273: 1085-90.

Figure & Scheme captions

Scheme 1. The synthesis route and structures of dye molecular **AHP** and **AHPN**.

Figure 1. pH-Dependent fluorescence responses of **AHP** (2×10^{-5} M) in distilled water upon excitation at 450 nm (pH from 2 to 13) $\lambda_{\text{max-em}}=558$ nm.

Figure 2. Absorbance spectra change of **AHPN** (20 μM) and upon the addition of various metal ions (4.0×10^{-3} M) in water. Inset: Photographs of samples show that the change in color of the solution of sensor **AHPN** after addition of Cu^{2+} and other metal ions (5 equiv.) in water under irradiation with visible light.

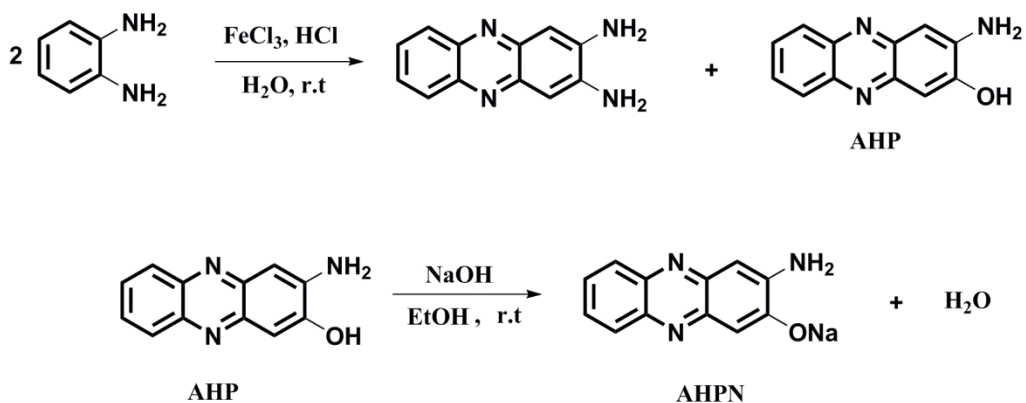
Figure 3. Fluorescence changes of **AHPN** (20 μM) upon addition of Cu^{2+} and other different perchlorate salts of metal ions (4.0×10^{-3} M) in water (excitation wavelength = 450 nm). Inset: Photographs of samples show that the change in color of the solution of sensor **AHPN** after addition of Cu^{2+} and other metal ions (5 equiv.) in water under irradiation with a UV lamp at 365 nm.

Figure 4. Partial ^1H NMR titration spectra (400 MHz) of 0.05 mol/L **AHPN** with various equivalents of Cu^{2+} in $\text{DMSO}-d_6$ solution (0, 0.1, 0.3, 0.5, 1.0 and 2.0 equiv).

Figure 5. Proposed binding model of dye molecule **AHPN** with Cu^{2+} .

Figure 6. The HOMO–LUMO energy gaps for **AHPN** (left) and **AHPN-Cu** (right).

Figure 7. Photographs of **AHPN** and added Cu^{2+} in fresh double distilled water under natural light and irradiation with the UV lamp at 365 nm (from top to bottom).



Scheme 1. The synthesis route and structures of dye molecular **AHP** and **AHPN**.

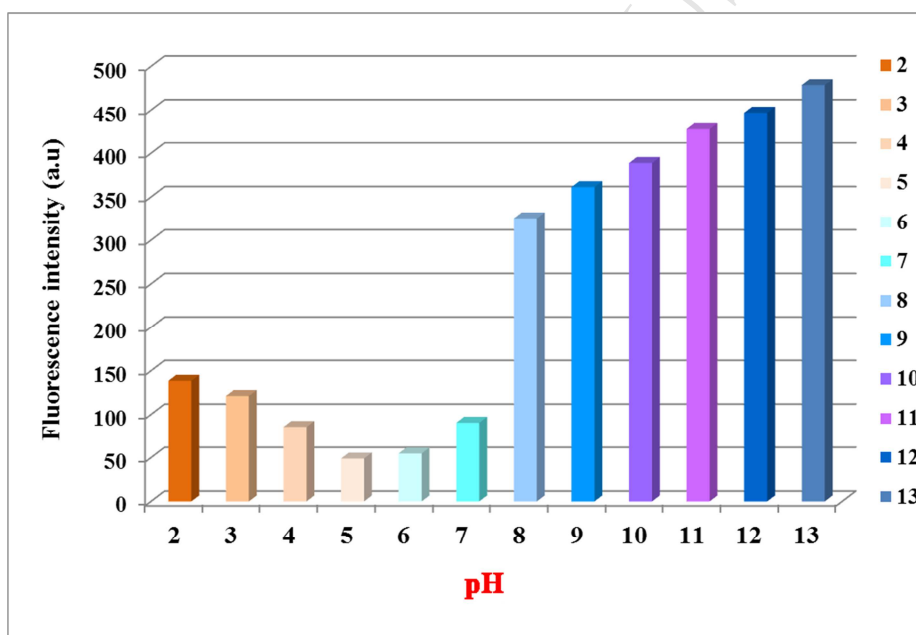


Figure 1. pH-Dependent fluorescence responses of **AHP** (2×10^{-5} M) in distilled water upon excitation at 450 nm (pH from 2 to 13) $\lambda_{\text{max-em}}=558$ nm.

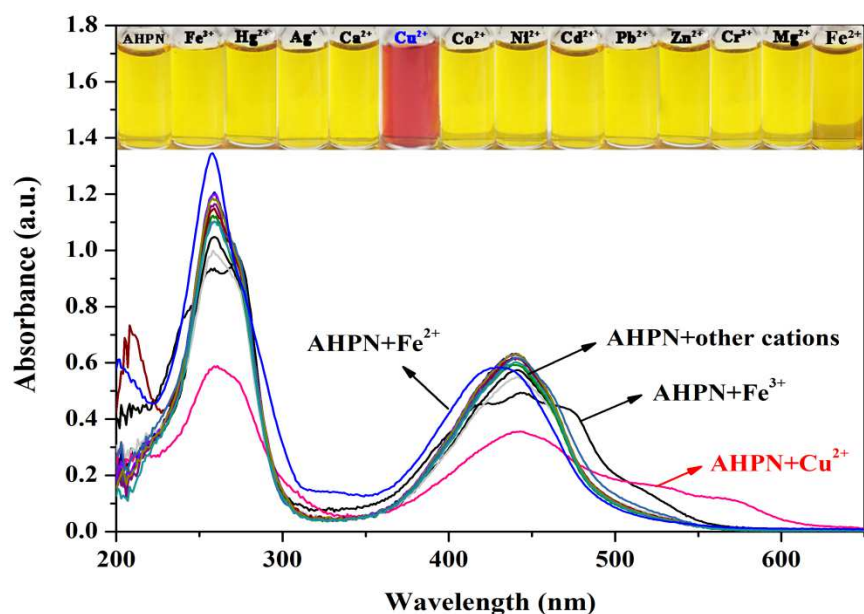


Figure 2. Absorbance spectra change of **AHPN** (20 μM) and upon the addition of various metal ions (4.0×10^{-3} M) in water. Inset: Photographs of samples show that the change in color of the solution of sensor **AHPN** after addition of Cu^{2+} and other metal ions (5 equiv.) in water under irradiation with visible light.

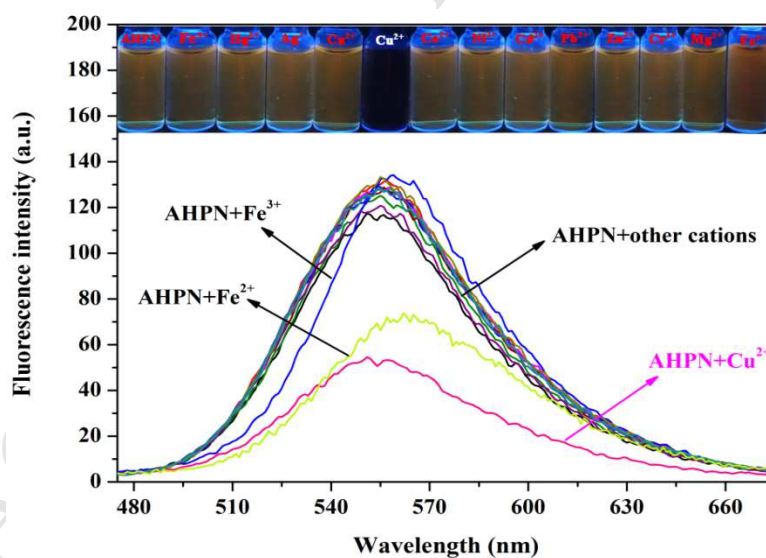


Figure 3. Fluorescence changes of **AHPN** (20 μM) upon addition of Cu^{2+} and other different perchlorate salts of metal ions (4.0×10^{-3} M) in water (excitation wavelength = 450 nm). Inset: Photographs of samples show that the change in color of the solution of sensor **AHPN** after addition of Cu^{2+} and other metal ions (5 equiv.) in water under irradiation with a UV lamp at 365 nm.

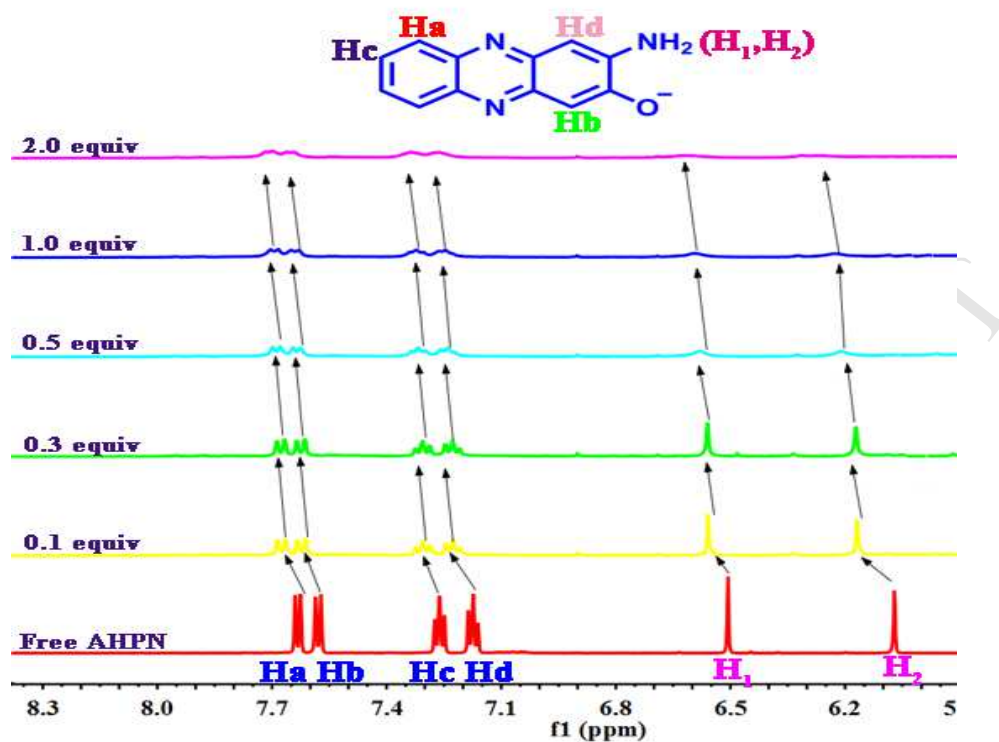


Figure 4. Partial ^1H NMR titration spectra (400 MHz) of 0.05 mol/L AHPN with various equivalents of Cu^{2+} in $\text{DMSO}-d_6$ solution (0, 0.1, 0.3, 0.5, 1.0 and 2.0 equiv).

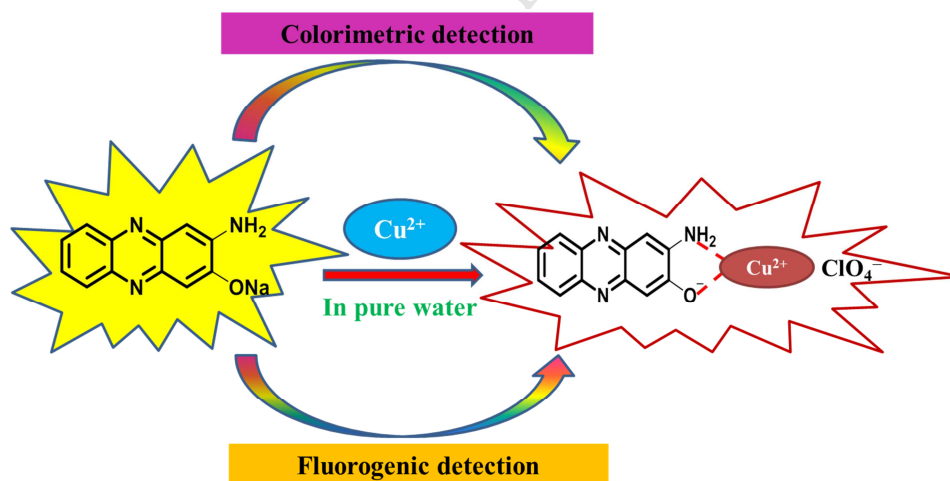


Figure 5. Proposed binding model of dye molecule AHPN with Cu^{2+} .

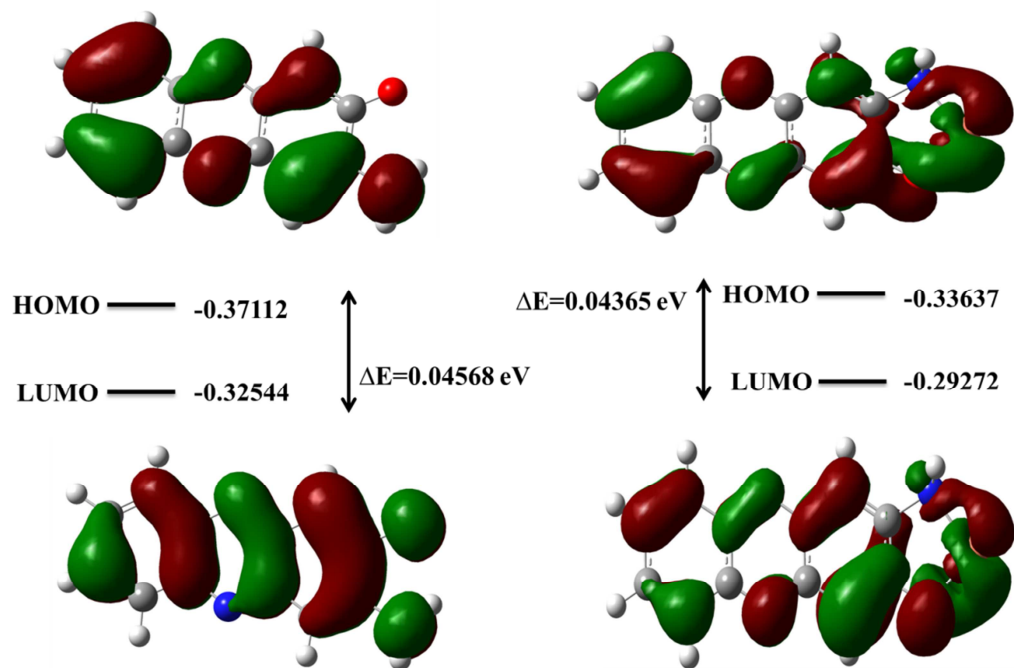


Figure 6. The HOMO-LUMO energy gaps for AHPN (left) and AHPN-Cu (right).

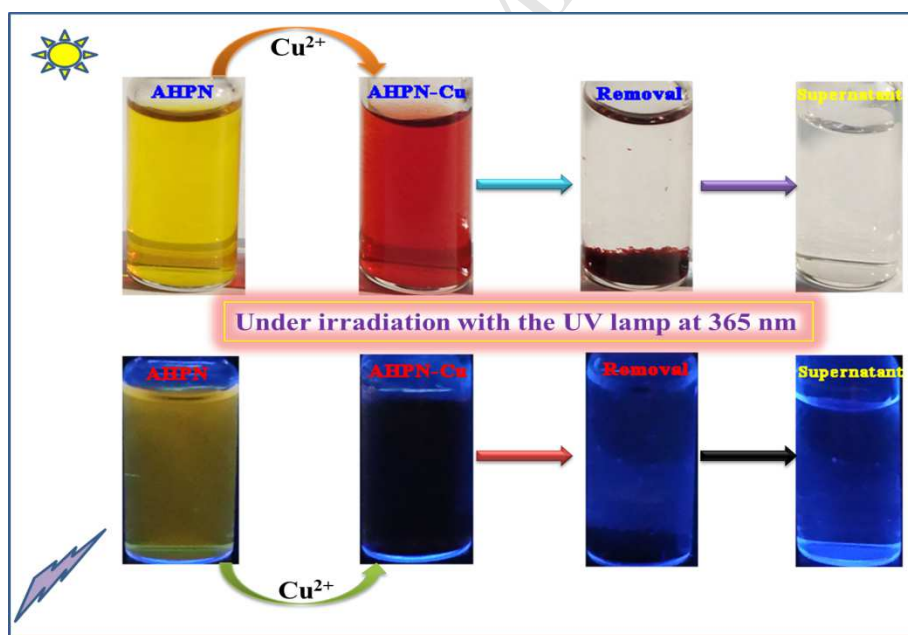


Figure 7. Photographs of AHPN and added Cu^{2+} in fresh double distilled water under natural light and irradiation with the UV lamp at 365 nm (from top to bottom).

Highlights

1. A water-soluble phenazine dye (**AHPN**) was synthesized.
2. **AHPN** can detect Cu^{2+} with colorimetric/fluorogenic in water and plant samples.
3. **AHPN** can effectively remove Cu^{2+} in natural water samples.
4. The test strips based on phenazine dye **AHPN** also were fabricated.